Impedance-based Inertia Estimation of Power Systems using Admittance Scanning Technique

Dinithi Senarath
Electrical Engineering & Robotics
Queensland University of Technology
Brisbane, Australia
dinithisandunika.senarath@hdr.qut.edu.au

Yateendra Mishra
Electrical Engineering & Robotics
Queensland University of Technology
Brisbane, Australia
yateendra.mishra@qut.edu.au

Mahinda Vilathgamuwa
Electrical Engineering & Robotics
Queensland University of Technology
Brisbane, Australia
mahinda.vilathgamuwa@qut.edu.au

***Abstract*—The increasing penetration of inverter-based resources (IBRs) in modern power systems introduces significant challenges for grid stability and dynamic performance due to the absence of inherent physical inertia. Compared with synchronous generators, these resources lead to reduced system inertia, degraded frequency response, weaker voltage support, and lower short-circuit strength, which complicates dynamic analysis in IBR-dominated grids. This paper presents an inertia estimation method based on dynamic admittance scanning using the admittance scan tool developed by MathWorks. The proposed approach is validated for a synchronous machine and a grid-forming virtual synchronous machine (VSM)-based battery energy storage system (BESS), with the analysis explicitly highlighting the inherent limitations associated with each implementation. The results show that the method enables effective inertia characterization and frequency response assessment, supporting stability analysis, and could be used to support the operation of modern power systems with high IBR penetration.**

***Index Terms*—Admittance scanning, Inertia, Power system stability, Inverter-based resources, Stability assessment.**

I. Introduction

The global power sector is undergoing a rapid transformation driven by increasing electricity demand and the transition toward sustainable energy systems. Electrification of transportation, expansion of data centers, urban development, and rising use of air conditioning and electric heating have significantly increased power consumption. The International Energy Agency (IEA) reported a 4.3% rise in global electricity demand in 2024, compared to 2.5% in 2023, indicating accelerated system loading [1].

At the same time, renewable energy deployment has expanded in response to climate change, fossil fuel depletion, and international policy commitments such as the Paris Agreement [2]. Global renewable capacity increased by 18% in 2024, with 741 gigawatts (GW) of new installations, representing the highest annual growth on record. China alone contributed 60.2% of this expansion. In addition, 2024 became the hottest year on record, with global temperatures exceeding 1.5°C above pre-industrial levels, reinforcing the role of renewable energy as both a climate mitigation measure and an essential infrastructure asset. According to the REN21 Global Status Report 2025, global electricity generation reached approximately 30.9 thousand terawatt hours (TWh) in 2024, with renewables accounting for 31.9% of total generation [3].

Wind, solar photovoltaic (PV), and BESSs now dominate new generation capacity additions worldwide. Renewable energy use across the power, heat, and transport sectors is projected to grow by nearly 60% between 2024 and 2030, increasing the renewable share in final energy consumption from 13% in 2023 to nearly 20% by 2030 [4].

Despite these benefits, the transition introduces significant operational challenges. Most renewable sources are IBRs that connect to the grid through power electronic interfaces and lack the inherent rotational inertia of synchronous generators [5]. As synchronous generation is displaced, system inertia declines, a trend already observed in the Australian National Electricity Market (NEM), the Electric Reliability Council of Texas (ERCOT), and several European power systems [6], [7].

Reduced inertia increases the risk of frequency instability. Disturbances such as generation outages or load changes lead to higher rates of change of frequency (RoCoF), which can trigger protection malfunctions, load shedding, and widespread outages [8]. These challenges highlight the need for advanced stability assessment techniques for inverter-dominated power systems. This paper applies the admittance scan method for system inertia estimation. It reviews stability assessment approaches for IBRs, introduces the admittance scanning technique to analyze frequency response characteristics, and presents impedance-based inertia estimation with representative case studies.

II. Stability Assessment Methods for Inverter-based Power Systems

Stability assessment in power systems relies on analytical, numerical, and data-driven methods to evaluate system behavior under varying operating conditions. Among these, impedance- and admittance-based techniques have proven particularly effective for small signal and dynamic stability analysis of inverter-dominated systems, alongside alternative approaches such as eigenvalue-based, measurement-based, and hybrid methods. Unlike state space methods that require full knowledge of inverter control structures and differential models that are often unavailable due to manufacturer restrictions, impedance-based analysis treats the inverter as a black box. By applying small signal current or voltage perturbations and observing the corresponding voltage or current responses,

979-8-3315-8138-1

dynamic impedance or admittance characteristics can be identified. These models provide stability insights comparable to conventional eigenvalue analysis while avoiding dependence on proprietary information, making impedance-based stability assessment (IBSA) well-suited for IBR-dominated power systems [9], [10].

III. Admittance Scanning Technique

A. *MathWorks Admittance Scan Tool*

Admittance scanning is a frequency domain analysis method implemented in MATLAB Simulink within the Renewable Energy Integration Design with Simscape repository. It enables systematic identification of the small signal admittance of grid-forming (GFM) and grid-following (GFL) inverters over user-defined frequency ranges using calibrated perturbation injection. This approach supports repeatable characterization of inverter dynamic behavior and facilitates the identification of oscillatory modes through Bode plot analysis, eigenvalue tracking, and cross-coupling assessment in IBR-dominated power systems.

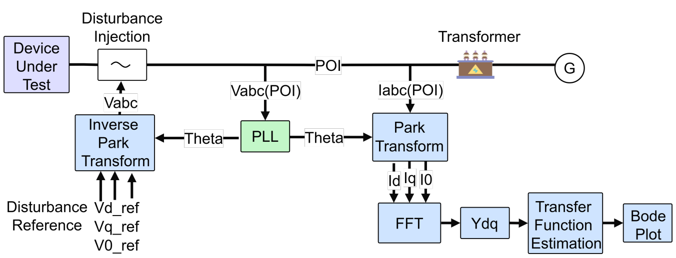

Fig. 1. Admittance Scan Tool Configuration

The admittance scan block characterizes the system by injecting a pseudo-random binary sequence (PRBS) voltage disturbance, which substantially reduces testing time compared with conventional sinusoidal frequency scanning that requires numerous single-frequency experiments. The excitation strength along the *dq*-axes can be adjusted by tuning the disturbance magnitude (V_d and V_q) in per unit, the frequency vector, the sampling time, and the injection intervals. A phase-locked loop (PLL) continuously tracks the grid's steady-state frequency and phase angle, ensuring accurate reference alignment and enabling reliable transformation of measured three-phase voltages and currents into *dq*-frame quantities.

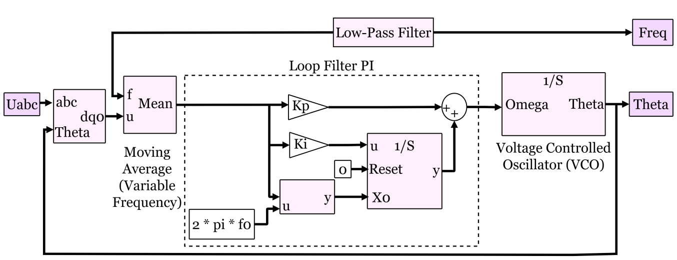

Fig. 2. Block diagram of a PLL block used in admittance scan tool

Using the PLL-based phase angle, the scan tool generates small signal voltage perturbations in the *dq*-frame and transforms them into *abc* phase voltages for series injection. The measured responses are processed using fast Fourier transform (FFT) to obtain frequency response data (FRD), which are reconstructed at discrete frequencies through spectral estimation. A state space model is first identified using N4SID (Numerical algorithms for Subspace State Space System IDentification) based on Hankel matrices formed from input-output data and is subsequently refined via nonlinear least squares optimization (`lsqnonlin`) to minimize the mismatch between measured and fitted frequency responses. The selected model order determines the number of poles and zeros in the transfer function, with higher orders improving the representation of low-frequency electromechanical dynamics at the expense of increased computational effort. The choice of model order is therefore application dependent and requires careful tuning.

The resulting *dq*-frame admittance matrix Y consists of four transfer functions (Y_{dd}, Y_{dq}, Y_{qd}, and Y_{qq}) that describe the frequency-dependent voltage-current relationship of the device under test. The diagonal terms represent self-admittances along the *d*- and *q*-axes, while the off-diagonal terms capture cross-coupling effects between the axes. This full representation enables the identification of mode-dependent interactions and frequency-dependent coupling phenomena that are critical for inertia estimation and small signal stability analysis in inverter-based power systems. The extracted admittance matrix supports IBSA using Nyquist and Bode plots. Comparing multiple scans under different operating conditions enables the identification of admittance variations and resonance shifts. In this work, such comparisons are performed using a finite set of discrete operating scenarios, and the resulting resonance frequencies are evaluated on a per-scenario basis [11].

B. *Verification of Scan Tool Applicability for Synchronous Machines*

Establishing confidence in admittance scan methodologies for emerging grid assets requires validation against well-understood reference systems, particularly classical synchronous machines. By applying the same admittance extraction procedures to synchronous generator models, this work demonstrates that the scan tool accurately reproduces known system behavior, thereby reinforcing the credibility of IBSA in IBR-dominated power systems. Such validation is essential given the continued coexistence of synchronous generation and increasing IBR penetration in practical power grids. Accordingly, the validation process begins with admittance scanning of a single synchronous machine system, as shown in Fig. 3.

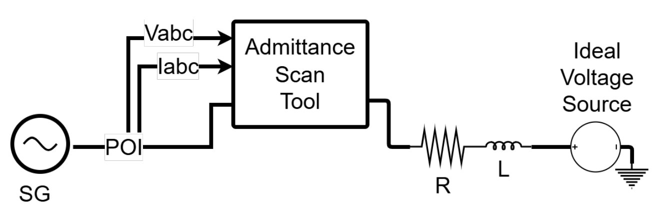

Fig. 3. Scan tool verification for a synchronous machine

979-8-3315-8138-1

According to Fig. 4, the admittance transfer function estimated by the scan tool closely matches the analytical transfer function derived from fundamental admittance calculations.

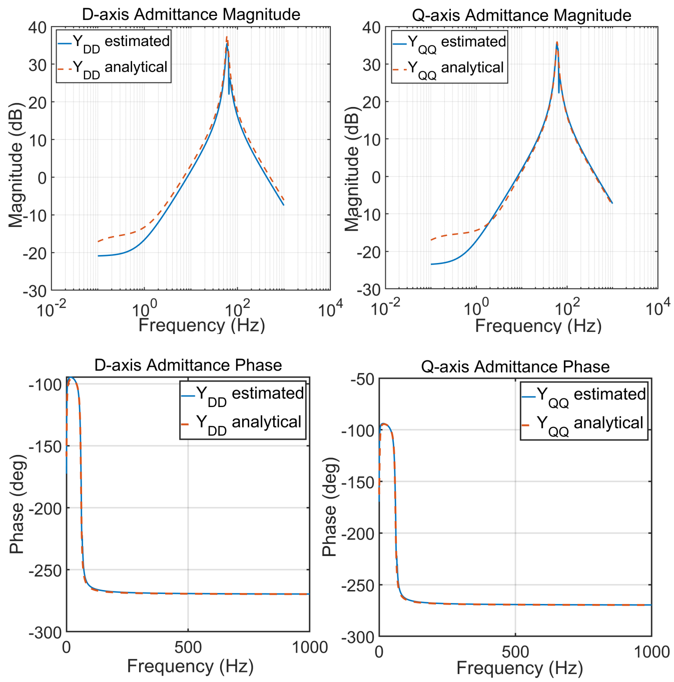

Fig. 4. Comparison of estimated and analytical admittance transfer function results

IV. Frequency Response Characterization

Building upon the admittance scan measurements of the device admittances at the point of interconnection (POI) described in Section III, this work applies the impedance-based frequency response transfer function, $FR(s)$ approach to estimate the nodal inertia. The measured *dq*-frame admittance matrix characterizes the dynamic interaction between the device and the surrounding network. The resonance frequency inherent in the device admittance is related to the system inertia through the $FR(s)$ metric, which links frequency perturbations at the POI, $f_{sr}(s)$, to active power perturbations, $p_{sr}(s)$ as shown in (1). Following established procedures in [12], and [13], the characteristic resonance frequencies identified in the admittance spectra enable the estimation of the inertia parameters at the node of interconnection.

$$FR(s) = \frac{f_{sr}(s)}{p_{sr}(s)} \approx \frac{2}{3u_{sd0}} \cdot \frac{1}{U_s} \cdot \frac{s}{2\pi} \cdot Z_{qd}(s) \tag{1}$$

It is assumed that the PLL used within the admittance scan tool is tuned such that, over the frequency range employed for inertia estimation, its closed-loop response is approximately unity and does not introduce dominant dynamic shaping. This condition is enforced by selecting PLL parameters that yield an effective bandwidth significantly higher than the resonance frequency used for inertia extraction.

Consequently, (1) directly relates the off-diagonal impedance element $Z_{qd}(s)$ to the frequency response, enabling inertia extraction from the admittance scan measurements without requiring detailed knowledge of the internal device control structures.

Analysis of $FR(s)$ reveals that the resonance point corresponds to a series resonance condition between the equivalent capacitance arising from the nodal inertia and the equivalent line inductance at the perturbation injection node, similar to a series resonant circuit with inductance, capacitance, and resistance [12]. This physical interpretation enables the direct extraction of the system inertia at the POI from the measured impedance data without requiring explicit knowledge of the individual generator parameters.

The series resonance frequency ω_H is governed by the fundamental LC resonance relationship, representing the natural oscillatory mode of the inertial response interacting with the network impedance. The resonance condition is expressed as:

$$\omega_H = \frac{1}{\sqrt{L_{eq} C_{H,eq}}} \tag{2}$$

where L_{eq} represents the equivalent inductance of the transmission network, and $C_{H,eq}$ represents the equivalent capacitance attributable to rotational inertia.

The identification of this resonance frequency from the $FR(s)$ characterization forms the basis for inertia estimation.

V. Impedance-Based Inertia Estimation

The inertia constant H, which characterizes the dynamic response capability of a synchronous machine, is defined as the ratio of the kinetic energy stored at the nominal speed to the generator's MVA capacity [14]. It can also be further expressed mathematically in terms of the moment of inertia J and the nominal system parameters as follows:

$$H = \frac{J\omega_N^2}{2S_N} \tag{3}$$

where ω_N is the nominal angular frequency, and S_N represents the nominal apparent power rating.

By combining the resonance condition given in (2) with the inertia definition in (3), and incorporating the relationship between the equivalent inertia and the capacitance, as discussed in [12], the nodal inertia H_n at bus n can be expressed as follows:

$$H_n = \frac{u_N^2}{2S_N L_{eq} \omega_H^2} \tag{4}$$

where u_N denotes the nominal voltage at the measurement bus and L_{eq} represents the equivalent line inductance.

This formulation provides a practical and non-invasive method for inertia estimation by identifying the characteristic resonance frequency ω_H from the $FR(s)$ response curve and by applying the known transmission network parameters. The approach is particularly valuable for black-box characterization of commercial IBRs and system-level inertia assessment in aggregated networks, where system parameters may be unavailable or time-varying.

979-8-3315-8138-1

A. Case Study

Since modern power systems still include conventional synchronous generators, the proposed impedance-based inertia estimation method using admittance scanning was validated on a single machine system rated at 50 MVA with an inertia constant of 6.5 s. The $Z_{qd}(s)$ component extracted from the scanned admittance data was used to derive the magnitude response $FR(s)$ according to (1), from which the resonance frequency was identified. The estimated resonance frequency exhibited strong sensitivity to the admittance scan configuration. In particular, the selected admittance model order and the proportional and integral gains of the PLL loop filter of the scan tool had a significant impact on the resulting $FR(s)$. Changes in these parameters shifted the resonance location, leading to corresponding variations in the estimated inertia. Fig. 5 illustrates the dependence of $FR(s)$ on the selected order of the admittance fitting model.

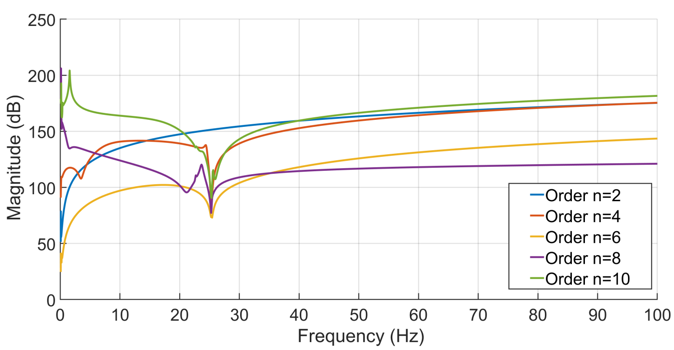

Fig. 5. Effect of model order on $FR(s)$ characterization

The parametric sensitivity of the frequency response $FR(s)$ to the PLL controller gains of the scan tool is shown in Fig. 6 and Fig. 7. Fig. 6 shows the effect of varying K_p while keeping K_i fixed at 3000, whereas Fig. 7 presents the effect of changing K_i with K_p fixed at 150. The results indicate that increasing the PLL gains leads to systematic shifts in the resonance frequency and corresponding changes in the magnitude of $FR(s)$, highlighting the strong dependence of the frequency response characteristics on the selected PLL parameters of the admittance scan tool.

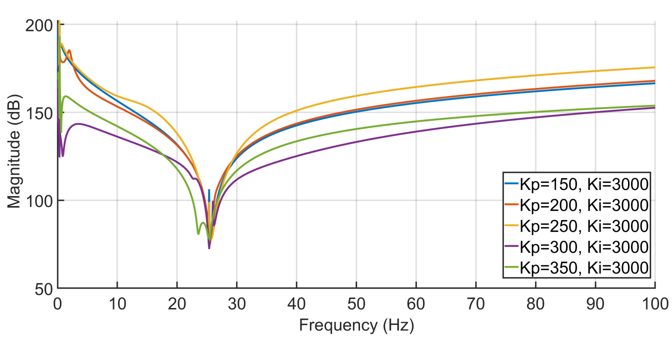

Fig. 6. Effect of K_p on $FR(s)$ when K_i Fixed

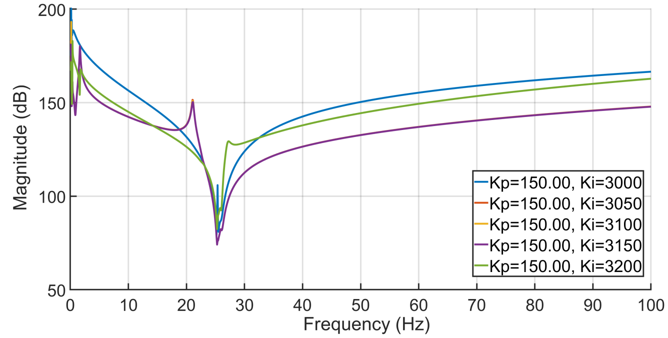

Fig. 7. Effect of K_i on $FR(s)$ when K_p Fixed

To minimize PLL-induced distortion while preserving resonance resolution, optimal PLL tuning must be performed. For the parameters $K_p = 154.5$ and $K_i = 3060$, with a model order of 10, the characteristic resonance frequency of the test system was identified as 1.54381 Hz, as shown in Fig. 8. Based on (4), the estimated inertia constant is 6.68 s, which closely matches the machine nameplate inertia constant of 6.5 s.

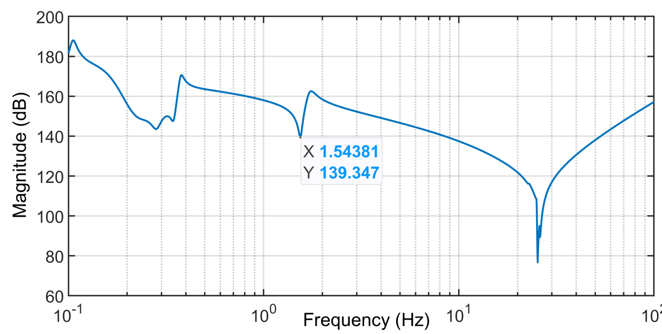

Fig. 8. Magnitude response curve of $FR(s)$ at the POI of a single-machine system

The same procedure was applied to estimate the nodal inertia at bus 1 of a two-area power system with a double-loop tie line and a rated system voltage of 230 kV. Each area contained two synchronous machines rated at 50 MVA with an inertia constant of 6.5 s. The admittance scan was performed using the MathWorks admittance scan tool to obtain the admittance of the d- and q-axes and extract the component $Z_{qd}(s)$ for $FR(s)$ characterization. Fig. 9 shows the magnitude response of the $FR(s)$ curve, where the resonant frequency was identified as 0.459019 Hz, which was then used for inertia estimation.

Based on (4), the estimated nodal inertia at bus 1 is 6.6416 s for a model order of 10 with K_p and K_i set to 150 and 750, respectively.

Applying the same approach to a system with a VSM-based GFM controller and a BESS, the inertia at the POI was estimated. As shown in Fig. 10, a resonance frequency of 5.85 Hz was identified, resulting in an estimated inertia of 2.8934 s when the VSM inertia is set to 3 s, and for the selected admittance scan tool parameters, a model order of 12 with K_p and K_i values of 178 and 15800, respectively.

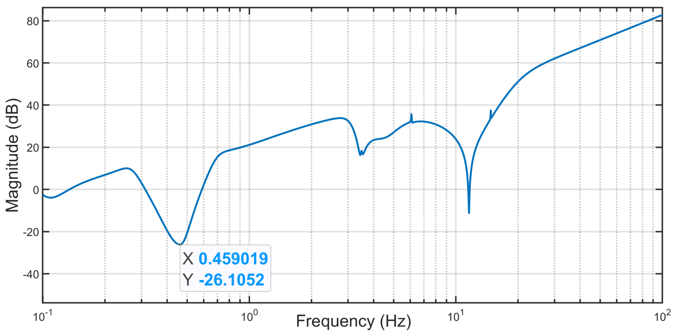

Fig. 9. Magnitude response curve of $FR(s)$ at bus 1 of the two-area system

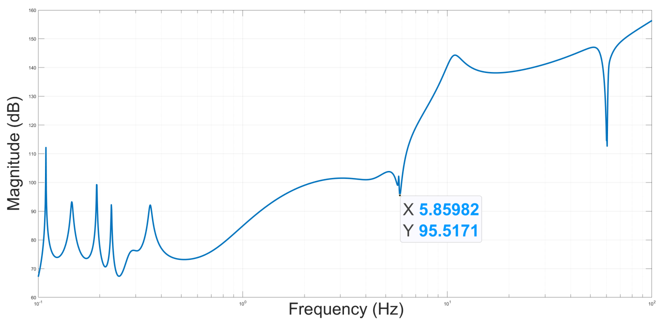

Fig. 10. Magnitude response curve of $FR(s)$ at bus 1 of the GFM BESS system with VSM Control

VI. Conclusion

This paper examines the use of an admittance scan tool combined with impedance-based frequency response analysis for inertia estimation in modern power systems. As an initial step, the method is applied separately to a synchronous generator and a VSM control-based GFM with a BESS in order to first verify its feasibility and applicability for each source type in isolation. This separation allows the estimation results to be directly linked to either physical electromechanical inertia in synchronous machines or control-induced virtual inertia in GFM converters, without the added complexity of interaction effects.

Numerical case studies show close agreement between the estimated and assigned inertia values for both source types when analyzed individually, confirming the applicability of the proposed approach for both synchronous machines and GFM converter scenarios. The admittance extraction framework enables a repeatable and parameter-controlled characterization that can be readily integrated into grid stability analysis workflows. At the same time, the extracted frequency response is shown to be highly sensitive to the selected admittance fitting model order and the PLL gains of the admittance scan tool, thereby highlighting the limitations of the proposed method. While this sensitivity supports detailed dynamic characterization, insufficient calibration may introduce artificial damping and distort electromechanical resonance features.

These findings underscore the necessity for judicious benchmarking and systematic guidelines to ensure consistent and reliable inertia estimation. Future work will focus on developing structured procedures for model order selection and PLL gain tuning, ensuring that the proposed method remains reliable across a wide range of operating conditions. Building on the separate validation of synchronous generators and GFM converters, subsequent studies will extend the analysis to mixed systems that include synchronous generators as well as GFM and GFL resources in order to evaluate the practical applicability of the approach in realistic power system environments.

References

[1] IEA, "Global Energy Review 2025 – Analysis," International Energy Agency, Tech. Rep., Mar. 2025. [Online]. Available: https://www.iea.org/reports/global-energy-review-2025
[2] UNFCC, "The Paris Agreement | UNFCCC." [Online]. Available: https://unfccc.int/process-and-meetings/the-paris-agreement
[3] REN21, "GSR 2025 | Global Overview." [Online]. Available: https://www.ren21.net/gsr-2025/global_overview/
[4] IEA, "Global overview – Renewables 2024 – Analysis." [Online]. Available: https://www.iea.org/reports/renewables-2024/global-overview
[5] A. Ulbig, T. S. Borsche, and G. Andersson, "Impact of Low Rotational Inertia on Power System Stability and Operation," *IFAC Proceedings Volumes*, vol. 47, no. 3, pp. 7290–7297, Jan. 2014.
[6] F. Milano, F. Dörfler, G. Hug, D. J. Hill, and G. Verbič, "Foundations and Challenges of Low-Inertia Systems (Invited Paper)," in *2018 Power Systems Computation Conference (PSCC)*, Jun. 2018, pp. 1–25.
[7] J. Morren, S. de Haan, W. Kling, and J. Ferreira, "Wind turbines emulating inertia and supporting primary frequency control," *IEEE Transactions on Power Systems*, vol. 21, no. 1, pp. 433–434, Feb. 2006.
[8] P. Kundur, *Power system stability and control*. McGraw-Hill, 1994.
[9] A. Intriago, A. Paspatis, F. Liberati, and C. Konstantinou, "Admittance Identification of Grid-Forming Inverters Using Time and Frequency-Domain Techniques," Apr. 2025, arXiv:2504.17512 [eess]. [Online]. Available: http://arxiv.org/abs/2504.17512
[10] S. C. Das, L. Saravana, L. M. Vu, M. Bui, T. Vu, J. Zhang, and T. Ortmeyer, "A Survey on IBR Penetrated Power System Stability Analysis Using Frequency Scanning," Jan. 2025, arXiv:2501.08516 [eess].
[11] MathWorks Simscape Team (2026), "Renewable Energy Integration Design with Simscape," Feb. 2026. [Online]. Available: https://github.com/simscape/Renewable-Energy-Integration-Simscape/releases/tag/25.1.1.2
[12] W. Zhang, Y. Wen, and C. Chung, "Impedance-Based Online Estimation of Nodal Inertia and Primary Frequency Regulation Capability," *IEEE Transactions on Power Systems*, vol. 38, no. 3, pp. 2748–2760, May 2023, conference Name: IEEE Transactions on Power Systems.
[13] S. Shah and V. Gevorgian, "Impedance-Based Characterization of Power System Frequency Response," in *2019 IEEE Power & Energy Society General Meeting (PESGM)*, Aug. 2019, pp. 1–5.
[14] AEMO, "Inertia in the NEM explained," Mar. 2023. [Online]. Available: https://www.aemo.com.au/-/media/files/initiatives/engineering-framework/2023/inertia-in-the-nem-explained.pdf

979-8-3315-8138-1